





Wideband evaluation of two types of slow-wave microstrip lines

D. Wang,  F. Polat,  H. Tesmer, 
and R. Jakoby 

Institute for Microwave Engineering and Photonics, Technische Universität Darmstadt, Darmstadt, 64283, Germany (E-mail: ersin.polat@tu-darmstadt.de, henning.tesmer@tu-darmstadt.de, rolf.jakoby@tu-darmstadt.de)

✉ Email: wang@imp.tu-darmstadt.de

The design, characterization and comparison of two widely used approaches in realizing slow-wave effect on microstrip transmission lines, that is stub loaded and defected ground structure loaded microstrip lines are presented in a wide bandwidth (10–67 GHz) for the first time. Transparent substrate and dielectric material are chosen to ease the alignment of electrode and ground plane. Thin dielectric layer are applied to make the comparison prominent. The results indicate that defected ground structure loaded microstrip line has better RF performance in terms of compactness and insertion loss than stub loaded method within the whole band especially in thin film applications.

Introduction: A transmission line (TL) is the fundamental and key component for RF systems. It is not only used in connecting RF components, but also in wavelength λ based millimetre wave (mmW) devices, such as branchline coupler [1, 2], interference based crossover [3], impedance transformer, virtual coupling [4], and delay line phase shifters and so forth. Therefore, TLs with high performance are crucial for advanced RF systems. Microstrip line (MSL) is being widely used in mmW systems, because of its planarity and cost effective fabrication, which makes MSL suitable for monolithic microwave integrated circuits (MMIC) as well as for high-speed digital PCB. Compared with waveguides, the drawbacks of MSLs are lower power handling capability and higher loss. Hence, MSL with high compactness, low loss and high power handling capacity would be of interesting.

Stub loaded high impedance microstrip line: Compared to a conventional homogeneous 50Ω MSL, high impedance line loaded with open ended stubs (L-MSL), as shown in Figure 1a, performs longer electrical length within the same physical length, which is referred to as slow-wave (SW) effect. This approach has been widely applied in miniaturizing microstrip devices [1, 2]. Its equivalent circuit is given in Figure 2a. Z_C and θ_C represent the characteristic line impedance and electrical length of

MSL, where Z_C normally equals to 50Ω . Similarly, Z_H and θ_H represent a high impedance line. C is the capacitance of the open ended stub. The equivalent characteristic impedance Z_E and electrical length θ_E of L-MSL loaded with two stubs can be derived from ABCD-matrix:

$$\mathbf{A}_C = \begin{bmatrix} \cos\theta_C & Z_C \sin\theta_C \\ \frac{1}{Z_C} \sin\theta_C & \cos\theta_C \end{bmatrix}, \quad \mathbf{A}_{\text{stub}} = \begin{bmatrix} 1 & 0 \\ \omega C & 1 \end{bmatrix}, \quad (1)$$

$$\mathbf{A}_C = \mathbf{A}_E = \mathbf{A}_{\text{stub}} \cdot \mathbf{A}_H \cdot \mathbf{A}_{\text{stub}}, \quad (2)$$

This gives:

$$Z_C \sin\theta_C = Z_H \sin\theta_H \quad (3)$$

$$\cos\theta_C = \cos\theta_H - \omega C Z_H \sin\theta_H, \quad (4)$$

The SW factor K is defined as:

$$K = \frac{\theta_C}{\theta_H}, \quad (5)$$

According to Equation (3), with $Z_C = 50 \Omega$, the achievable SW factor depends on the highest possible Z_H that can be realized by microstrip TL. Nevertheless, the highest achievable Z_H by narrowing the transmission line width W_{TL} is limited to be around 100Ω , which limits the SW effect. Moreover, such narrow line causes high metallic loss and low power handling capability which largely limits the applicability of the L-MSL.

Defected ground structure loaded microstrip line: Instead of L-MSL, defected ground structure (DGS) loaded microstrip line (DGS-MSL) is also found to be able to provide SW effect, while keeping a low level loss. The 3-dimensional view of a DGS-MSL with rectangular dumbbell shape etched lattice on the ground plane is shown in Figure 1b, and its equivalent circuit is shown in Figure 2b. DGS introduces serial inductance to the TL by disturbing the return current on ground plane. Z_L and θ_L represent a low impedance TL, and L is the inductance of the single DGS lattice. Considering

$$\mathbf{A}_{\text{DGS}} = \begin{bmatrix} 1 & \omega L \\ 0 & 1 \end{bmatrix}, \quad (6)$$

the SW effect equation

$$Z_L \sin\theta_C = Z_C \sin\theta_L \quad (7)$$

could be derived similarly to Equation (3). It is realized by using low impedance TL with $Z_L < Z_C$ such that W_3 is wider and leads to less loss than L-MSL. This is a big advantage especially in high frequency applications as well as in applications where MSLs are used with thin dielectrics of less than $20 \mu\text{m}$.

Fabrication and measurement: By periodically cascading the elements shown in Figure 1, L-MSL and DGS-MSL realized in suspended microstrip line topology are designed and optimized in CST Microwave Studio (CST), both having $Z_E = 50 \Omega$. The cross section and dimensions of the suspended microstrip structure are given in Figure 3. To ease the alignment between DGS and electrode, transparent AF32 glass from Schott GmbH with $\epsilon_r = 5.1$ and $\tan\delta = 0.01$ is chosen as the top and bottom substrate, on which electrode and ground are plated by using standard photo lithography process described in [5]. Two glass substrates are precisely aligned with a distance of $h_2 = 20 \mu\text{m}$ held by spacers. Then a fluid dielectric with $\epsilon_r = 2.4$ and $\tan\delta = 0.002$ is filled in. Besides, a conventional MSL without any loading method and thru-reflect-line (TRL) kits are fabricated together with the proposed demonstrators as reference TL and post de-embedding kits, respectively. A photograph of all the aforementioned devices is shown in Figure 4. Three DGS-MSLs with different lattice dimensions, but same total length, are fabricated. Detailed dimensions are given in Figure 1. In order to perform on-wafer measurements on suspend microstrip TL with fluid dielectric,

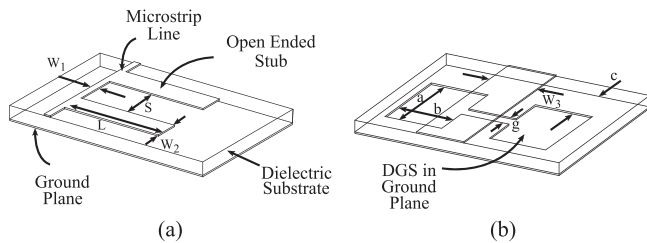


Fig. 1 3D view of (a) L-MSL and (b) DGS-MSL. Dimensions are given as: $W_1 = 10 \mu\text{m}$, $W_2 = 40 \mu\text{m}$, $L = 150 \mu\text{m}$, $S = 70 \mu\text{m}$; $W_3 = 100 \mu\text{m}$, $a = b = 120 \mu\text{m}$, $c = a/2 = 60 \mu\text{m}$, and $g = 20 \mu\text{m}$

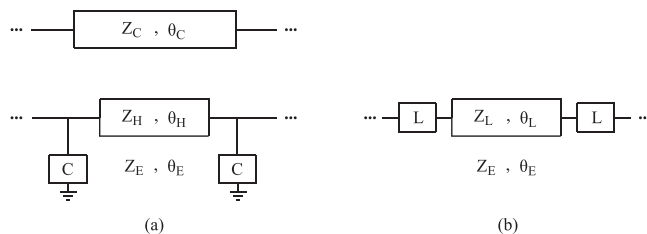


Fig. 2 Equivalent circuit of: (a) L-MSL and (b) DGS-MSL

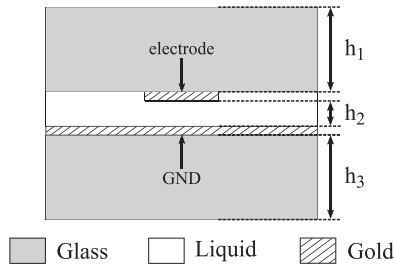


Fig. 3 Cross section of the suspended microstrip structure. Dimensions are given as: $h_1 = h_3 = 700 \mu\text{m}$, $h_2 = 20 \mu\text{m}$. GND and electrode are galvanic gold with $2 \mu\text{m}$ thickness

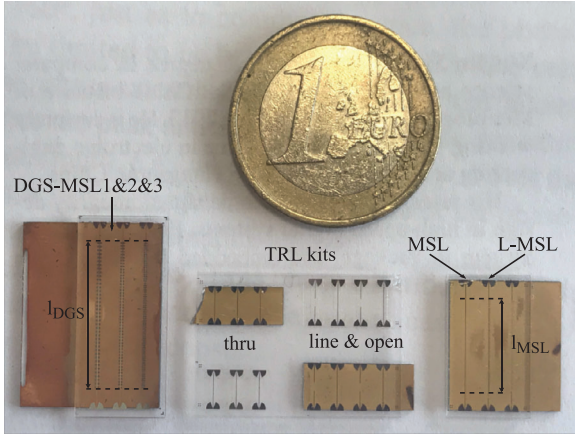


Fig. 4 Photograph of MSL, L-MSL, DGS-MSL1 ($a = b = 120 \mu\text{m}$), DGS-MSL2 ($a = b = 160 \mu\text{m}$), DGS-MSL3 ($a = b = 200 \mu\text{m}$) and TRL de-embedding kits. The dimensions are given as: $l_{DGS} = 16 \text{ mm}$ and $l_{MSL} = 10 \text{ mm}$

coplanar waveguide (CPW) contact pad with via-less CPW to MSL transition is designed [4]. First, all devices are measured from 100 MHz to 67 GHz, with two ports line-reflect-reflect-match (LRRM) probe tip calibration. Then, the influence of fixtures is removed by moving the reference plane directly to the device under test (DUT) by performing TRL de-embedding in Matlab. The reference planes after de-embedding are shown in Figure 4 as dashed lines.

The de-embedded measurement results of reference MSL, L-MSL, DGS-MSL1, DGS-MSL2 and DGS-MSL3, are shown in Figure 5 in terms of the absolute value of transmission coefficient $|S_{21}|$ and reflection coefficient $|S_{11}|$. All five demonstrators show broadband matching where $|S_{11}| < -15\text{dB}$. The raw measurement results before de-embedding also show good matching, indicating well-fabricated 50Ω devices, which is not plotted here for simplicity. Based on the de-embedded results, unit length loss α , propagation constant β , which represents compactness, and quality factor Q of the demonstrators are calculated and given in Figure 6. As an overall evaluation of SW effect and loss, Q is calculated as:

$$Q = \frac{\beta}{2\alpha}, \quad (8)$$

which represents how lossy the TL is. The higher the Q , the less loss generated by the TL. High Q transmission line is required in wavelength λ based passive mmW components, such as coupler, impedance transformer, delay line phase shifters and so forth, to minimize the dimension, loss and heating issues. Within their pass-bands, DGS-MSLs perform almost the same α as MSL, while L-MSL exhibits around twice the loss. Due to expected SW effect, DGS-MSLs and L-MSL all show higher β than MSL, among which DGS-MSL3 with largest etched area indicates the largest SW factor K of approximately 1.9 times that of MSL at 40 GHz. However, DGS-MSL3 performs low-pass feature and has a cut-off frequency at around 40 GHz due to the high lumped serial inductance compared to DGS-MSL1, which limits its pass-band according to Figure 5. In contrast, DGS-MSL2 with intermediate DGS size correspondingly indicates intermediate performance in terms of α , β as well

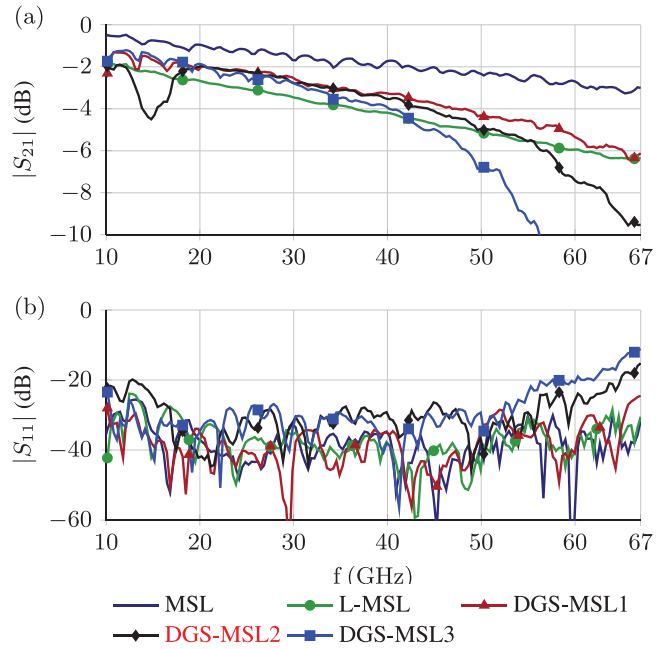


Fig. 5 De-embedded measurement results on amplitude of transmission coefficient $|S_{21}|$ and reflection coefficient $|S_{11}|$ of MSL, L-MSL, DGS-MSL1, DGS-MSL2 and DGS-MSL3

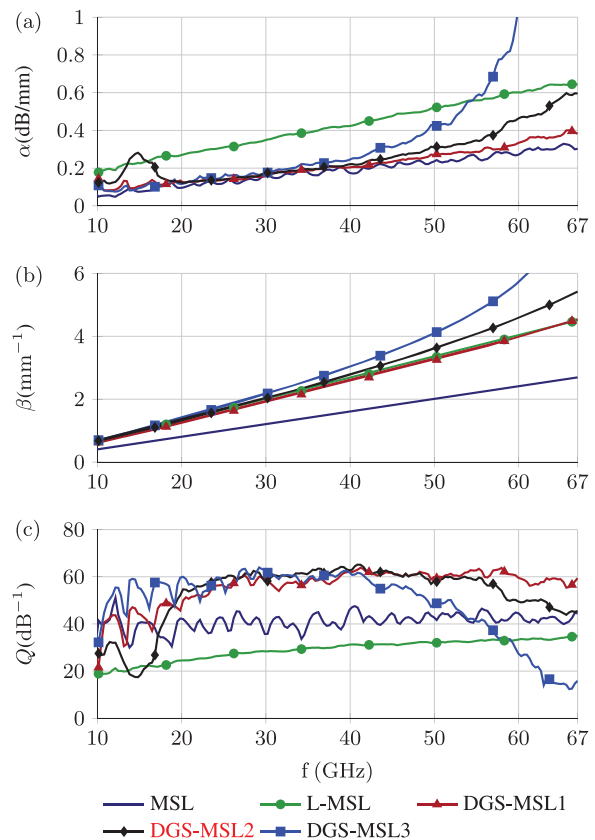


Fig. 6 Extracted parameters from de-embedded data: (a) unit length loss α , (b) propagation constant β and (c) quality factor Q of MSL, L-MSL, DGS-MSL1, DGS-MSL2 and DGS-MSL3

as bandwidth. DGS-MSL1 and L-MSL exhibit similar K . DGS-MSLs show an outstanding Q in their pass-bands. L-MSL has the lowest Q because it provides limited SW effect at the expense of drastically increased metallic loss. A comparison of L-MSL and DGS-MSL is summarized in Table. 1.

Table 1. Performance comparison of the two technologies

Technology	K	Q	f_{cutoff}	Fabrication effort	Versatility
L-MSL			✓	✓	
DGS-MSL	✓	✓			✓

✓ represents better performance

Conclusion: This work presents a comprehensive RF comparison of two types of slow-wave microstrip lines, namely L-MSL and DGS-MSL for the first time. A conventional MSL is fabricated as a reference for comparison. TRL de-embedding accurately extracts the electrical properties of the proposed demonstrators to validate the comparison. Compared to widely used L-MSL in miniaturizing microstrip TLs, DGS-MSL shows advantages of less loss, wider SW range and higher quality factor. In addition, the electrode width of DGS-MSL is wider than MSL, which increases its power handling capability and decreases the fabrication tolerance especially in thin film and high frequency applications. This gives a higher versatility of DGS-MSL. However, the etched dimension of DGS-MSL should be carefully chosen to provide suitable SW factor and passband: the higher the miniaturization, the lower the cut-off frequency of DGS-MSL. In addition, alignment of DGSs with electrode on thick, untransparent dielectric is challenging, especially when dimensions of TLs and DGS lattices are small which may cause degraded matching. While L-MSL with only one patterned metal layer is easier to be fabricated. L-MSL's disadvantage of high IL might be not critical in thick dielectric situations.

The conclusions above are instructional in choosing either of the methods to design compact and high performance mmW microstrip circuits.

Acknowledgements: This work was funded by the German Research Foundation DFG under Project-ID JA921/65-1.

Conflict of interest: The authors declare no conflict of interest.

Data availability statement: The data that support the findings of this study are available from the corresponding author, Dongwei Wang, upon reasonable request.

Credit statement: **Dongwei Wang:** conceptualization; investigation; methodology; validation; writing – original draft. **Ersin Polat:** writing – review and editing. **Henning Tesmer:** writing – review and editing. **Rolf Jakoby:** funding acquisition; project administration; supervision; writing – review and editing.

© 2021 The Authors. *Electronics Letters* published by John Wiley & Sons Ltd on behalf of The Institution of Engineering and Technology

This is an open access article under the terms of the Creative Commons Attribution License, which permits use, distribution and reproduction in any medium, provided the original work is properly cited.

Received: 18 October 2021 Accepted: 17 November 2021

doi: 10.1049/ell2.12389

References

- 1 Chun, Y.-H., Hong, J.-S.: Compact wide-band branch-line hybrids. *IEEE Trans. Microw. Theory* **54**, 704–709 (2006)
- 2 Gai, C., Jiao, Y., Zhao, Y.: Compact dual-band branch-line coupler with dual transmission lines. *IEEE Microwave Wireless Compon. Lett.* **26**(5), 325–327 May (2016)
- 3 Fai-Leung, W., Kwok-Keung, M.C.: A novel, planar, and compact crossover design for dual-band applications. *IEEE Trans. Microw. Theory* **59**, 568–573 (2011)
- 4 Zhu, L., Melde, K.L.: On-wafer measurement of microstrip-based circuits with a broadband vialess transition. *IEEE Trans. Advan. Packa.* **29**, 654–659 (2006)
- 5 Karabey, O.H., Gaebler, A., Strunck, S., Jakoby, R.: A 2-D electronically steered phased-array antenna with 2×2 elements in LC display technology. *IEEE Trans. Microw. Theory* **60**(5), 1297–1306 May (2012)